



Contents lists available at ScienceDirect

Journal of Environmental Management

journal homepage: www.elsevier.com/locate/jenvman

Research article

Simplified engineering design towards a competitive lipid-rich effluents valorization

Lucía Argiz^{a,*}, Ángeles Val del Río^a, David Correa-Galeote^{b,c}, Belén Rodelas^{b,c}, Anuska Mosquera-Corral^a^a CRETUS Institute, Department of Chemical Engineering, Universidade de Santiago de Compostela, 15782, Santiago de Compostela, Galicia, Spain^b Department of Microbiology, Faculty of Pharmacy, University of Granada, 18001, Granada, Andalucía, Spain^c Microbiology and Environmental Technology Section, Department of Microbiology, Faculty of Pharmacy, University of Granada, 18001, Granada, Andalucía, Spain

ARTICLE INFO

Keywords:

Bioprocess
Mixed microbial culture
Triacylglyceride
Polyhydroxyalkanoate
Waste lipids

ABSTRACT

Medium- and long-chain fatty acids and glycerol contained in the oily fraction of many food-industry effluents are excellent candidates to produce biobased high-value triacylglycerides (TAGs) and polyhydroxyalkanoates (PHAs). The typical process configuration for TAGs recovery from lipid-rich streams always includes two steps (culture enrichment plus storage compounds accumulation) whereas, for PHAs production, an additional pre-treatment of the substrate for the obtainment of soluble volatile fatty acids (VFAs) is required. To simplify the process, substrate hydrolysis, culture enrichment, and accumulation (TAG and PHA storage) were coupled here in a single sequencing batch reactor (SBR) operated under the double growth limitation strategy (DGL) and fed in pulses with industrial waste fish oil during the whole feast phase. When the SBR was operated in 12 h cycles, it was reached up to 51 wt % biopolymers after only 6 h of feast (TAG:PHA ratio of 50:51; 0.423 Cmmol_{BIOP}/Cmmol_S). Daily storage compound production was observed to be over 25% higher than the reached when enrichment and accumulation stages were carried in separate operational units. Increasing the feast phase length from 6 to 12 h (18 h cycle) negatively affected the DGL strategy performance and hence system storage capacity, which was recovered after also extending the famine phase in the same proportion (24 h cycle). Besides, the carbon influx during the feast phase was identified as a key operational parameter controlling storage compounds production and, together with the C/N ratio, culture selection. The different cycle configurations tested clearly modulated the total fungal abundances without no significant differences in the size of the bacterial populations. Several PHA and TAG producers were found in the mixed culture although the PHA and TAG productions were poorly associated with the increased relative abundances (RAs) of specific operational taxonomic units (OTUs).

Credit author statement

Lucía Argiz: investigation, writing-original draft, formal analysis, conceptualization; Ángeles Val del Río: formal analysis, validation, visualization, supervision, funding acquisition; David Correa-Galeote: validation, writing - review & editing, visualization; Belén Rodelas: validation, visualization, funding acquisition; Anuska Mosquera-Corral: validation, supervision, project administration, funding acquisition.

1. Introduction

The fish-canning industry is responsible for the generation of large volumes of high-loaded wastewater streams. In addition to being characterized by presenting relatively high salt concentrations, that degrade water quality hindering its direct reuse for industrial applications, these wastewater streams contain high concentrations of fat, oil, and grease (FOG) (Panagopoulos, 2021; Panagopoulos and Haralambous, 2020a, 2020b). Water pollution caused by these organic compounds has become a serious ecological issue. Consequently, several technologies (mostly physicochemical methods) have been applied in wastewater treatment plants (WWTPs) to separate FOG at the first stage of the

* Corresponding author.

E-mail address: luciaargiz.montes@usc.es (L. Argiz).<https://doi.org/10.1016/j.jenvman.2022.115433>

Received 7 February 2022; Received in revised form 14 May 2022; Accepted 26 May 2022

Available online 9 June 2022

0301-4797/© 2022 The Authors. Published by Elsevier Ltd. This is an open access article under the CC BY-NC license (<http://creativecommons.org/licenses/by-nc/4.0/>).

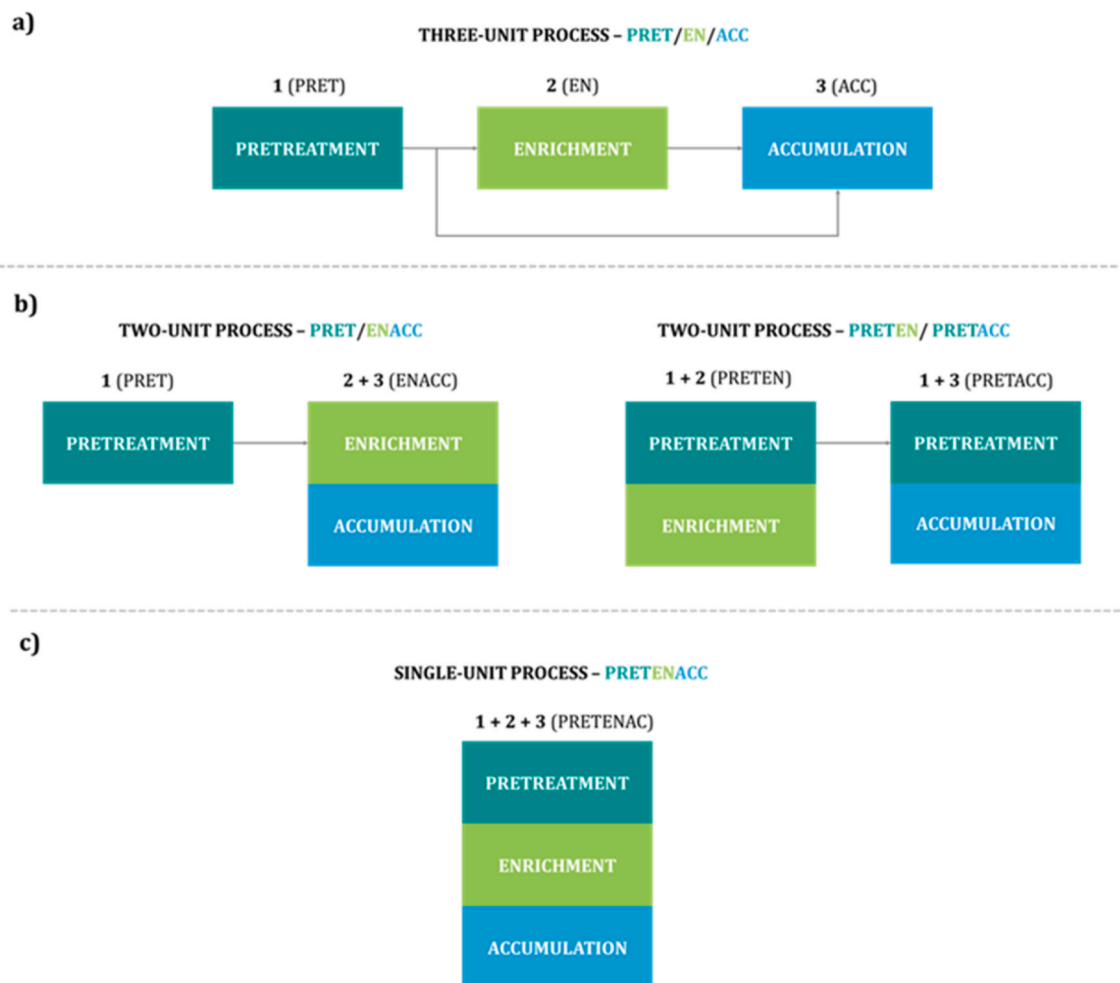


Fig. 1. Possible process configurations for TAG and PHA recovery using MMC biotechnologies. ACC (accumulation), EN (enrichment), ENACC (enrichment + accumulation), PRET (pretreatment), PRETACC (pretreatment + accumulation), PRETEN (pretreatment + enrichment), PRETENACC (pretreatment + enrichment + accumulation).

treatment to avoid blockages in the infrastructure, and the reduction of microbial activity in conventional biological treatment systems (Wallace et al., 2017; Yousefi et al., 2021).

Nowadays, reusing these residual lipids as possible raw materials presents high potential because of their disposal necessity, low cost, and expected constant increase in the future (Frkova et al., 2020). FOG is mainly composed by medium and long-chain fatty acids and glycerol (Husain et al., 2014), excellent precursors for the biological production of value-added, renewable, biodegradable, and bio-based triacylglycerides (TAGs) and polyhydroxyalkanoates (PHAs), the hallmark compounds accumulated in eukaryotes and prokaryotes, respectively (Alvarez et al., 2013; Garay et al., 2014). Microbial TAGs can be used for the production of third-generation biodiesel although they also present applications in industries such as agri-food (Bharathiraja et al., 2017) and the pharmaceutical (Alvarez and Steinbüchel, 2002). PHAs are polymers in the form of polyesters that are expected to substitute conventional plastics such as polypropylene (PP) and low-density polyethylene (LDPE) due to their similar properties (Kourmentza et al., 2017).

To date, lipid-rich waste streams valorization for TAGs and PHAs production was mainly focused on the use of pure strains (Chan et al., 2018; Herrero et al., 2018; Lopes da Silva et al., 2018; Riedel et al., 2015; Sangkharak et al., 2020; Surendran et al., 2020; Vastano et al., 2019). Studies concerning mixed microbial cultures (MMCs) are still very scarce and generally involve a three-unit process (Campanari et al., 2017; Gobi and Vadivelu, 2014; Md Din et al., 2006; Waller et al., 2012)

(PRET/EN/ACC, Fig. 1a): (1) fermentation of the lipid-rich substrate to obtain soluble and easily metabolizable organic acids (commonly volatile fatty acids (VFAs) suitable for their bioconversion into PHA) (PRET); (2) sequencing batch reactor (SBR) for the selection of a MMC with a high storage ability (EN); and (3) fed-batch reactor (FBR) for storage compounds maximization before their extraction and purification (ACC). To the best of the authors' knowledge, only Argiz et al. (2021a, 2021b) were able to recover TAGs and PHAs from a lipid-rich waste stream using a two-unit process with no need for substrate pretreatment. The carbon source was directly fed to SBR and FBR reactors, and simultaneously hydrolyzed in both units (PRETEN/PRETACC, Fig. 1b).

MMC are usually enriched under aerobic dynamic feeding (ADF) conditions in which the culture is subjected to cycles of excess/absence of carbon source (feast/famine (F/F) regime) (Kourmentza et al., 2017) creating a competitive advantage for those microorganisms capable of storing the substrate inside their cells as a reserve (Marang et al., 2016). Nonetheless, many industrial wastes/by-products used as feedstocks, such as FOG, present high carbon concentrations but a poor nutrient content being necessary their supplementation during culture selection (Oliveira et al., 2017). In these cases, it is possible to implement the double growth limitation strategy (DGL), in which carbon and nutrients are fed separately at the beginning of the feast and famine phases, respectively. This allows for a faster selection of a more efficient storing culture and for a higher intracellular accumulation at the end of the feast phase (Lorini et al., 2020; Oliveira et al., 2017; Silva et al., 2017), which

suggests the possibility of simplifying the process contributing towards its cost-efficiency. Thus, a separate accumulation unit might no longer be required if part of the biomass (with the highest achievable polymer content) is already harvested at the end of the feast phase (Kourmentza et al., 2017; Marang et al., 2016; Silva et al., 2017).

Nonetheless, it is necessary to optimize the enrichment at conditions maximizing accumulation. Otherwise, downstream-processing costs may increase as the maximum intracellular content obtained in the SBR is generally much lower than that obtained after the FBR (Marang et al., 2016). Zeng et al. (2018) studied the possibility of coupling the enrichment and accumulation steps in an SBR fed with VFAs (PRET/ENACC, Fig. 1b) by the combination of the DGL strategy with the so-called feed-on-demand control. Following the fact that pulsed feeding strongly improves accumulation due to avoiding the effect of substrate inhibition (Albuquerque et al., 2007), the carbon source was fed in small pulses during the feast phase based on the oxygen uptake rate. However, this feeding strategy might not be suitable when using non-pretreated complex substrates such as lipid-rich waste streams. Thus, these present a high immiscibility in water and a slow diffusivity requiring additional time to assure carbon source hydrolysis and its accessibility to the culture. Moreover, FOG substrates cause fouling and can ever degrade dissolved oxygen (DO) probes limiting their effectiveness when using complex control systems such as the one proposed by Zeng et al. (2018).

Therefore, previous studies demonstrated the feasibility on reducing the typical MMC valorization process from three to two units (PRETEN/PRETACC, and PRET/ENACC). However, the possibility of coupling substrate pretreatment, culture enrichment, and storage compounds accumulation in a single reactor was not explored so far. In this research work, a lipid-rich waste stream generated in the fish-canning industry was valorized in a single-unit process. For that purpose, it was combined the DGL strategy with operating the SBR during the feast phase as a typical accumulation FBR. That is to say, feeding pulses of small amounts of carbon source during an extended period in the absence of nitrogen according to DO profiles. Firstly, it was evaluated the feasibility of performing in a unique SBR the hydrolysis of the substrate (PRET), the enrichment of the culture (EN), and intracellular compounds accumulation maximization (ACC), (PRETENAC, Fig. 1c). Then, it was studied the effect of the cycle configuration and certain operational parameters on the single-unit process performance and the microbial culture diversity. Also, the structure and total abundance of the bacterial and fungal communities were monitored.

PRETENAC is expected to contribute to rendering TAG and PHA production more economically feasible. Thus, it comprises a simplified engineering design with reduced costs and easily maintained operational conditions based on the use of MMC biotechnologies in which complex feedstocks may be used as carbon sources.

2. Materials and methods

2.1. Sequencing batch reactor set-up

An SBR with a working volume of 10 L was inoculated with activated sludge from an urban WWTP located in Santiago de Compostela, Spain. This reactor was operated under the F/F regime in cycles of 12, 18, and 24 h implementing the enrichment DGL strategy via separated carbon and nitrogen feedings.

The carbon source consisted of the oily fraction of a fish-canning industry effluent from canned tuna production removed in the primary treatment of the factory WWTP (see the characterization in Table SI.1). It was fed in pulses during the whole feast phase to increase storage efficiency and avoid substrate inhibition (Albuquerque et al., 2007; Serafim et al., 2004). Pulses frequency was defined according to DO concentration profiles considering the need for carbon source addition once the substrate fed in the previous pulse was depleted (DO decreases due to carbon source consumption, and once it is depleted, DO

Table 1

Main operational conditions during periods I – VI.

Parameter	Period I	Period II	Period III	Period IV
Days of operation	Start-up – 57	57–95	96–160	161–190
Cycle length (h)	12	18	24	12
F/F length (h/h)	6/6	6/12	12/12	6/6
OLR (g COD/(L·d))	0.72–1.44	0.96	0.60	0.42
C influx feast phase (Cmmol/(L·h))	1.72–3.44	1.72	1.43	0.50
C/N (mg C-oleic acid/mg N-NH ₄ ⁺)	12.55 ± 0.37	11.42 ± 0.70	18.27 ± 1.38	9.89 ± 0.65
pH	6.88 ± 0.27	7.37 ± 0.22	7.61 ± 0.29	7.80 ± 0.25
sCOD end cycle (g/L)	92.04 ± 16.98	128.66 ± 24.00	72.63 ± 13.01	71.75 ± 17.91
TN end cycle (mg/L)	9.67 ± 3.97	15.91 ± 1.81	5.10 ± 1.49	5.68 ± 2.14
VSS end cycle (g/L)	0.38 ± 0.08	0.28 ± 0.08	0.22 ± 0.07	0.07 ± 0.02

C/N (carbon to nitrogen ratio), sCOD (soluble Chemical Oxygen Demand), F/F (feast/famine), OLR (Organic Loading Rate), TN (Total Nitrogen), VSS (Volatile Suspended Solids).

starts to rise). At the end of the feast phase, half of the volume of the reactor (5 L) containing biopolymer-rich biomass was withdrawn, and then it was added the same volume (5 L) of a nutrient solution containing nitrogen (Table SI.2) heralding the beginning of the famine phase.

The SBR was continuously aerated through a diffuser located at the bottom, which granted the complete mixture of the system, and the temperature was controlled at 30 ± 2 °C by a thermostatic bath (Techne Inc. USA). pH-value was controlled offline and maintained at almost neutral values by NaHCO₃ buffer addition in the nutrient's solution.

2.2. Operational periods

The SBR was operated for 190 days, subdivided into four operational periods (I – IV) (Table 1). In periods I – III the substrate was added in pulses and different cycle configurations were tested according to feast and famine phases length, which determined the total length of the cycle (12, 18, or 24 h) and the periods of presence/absence of carbon and nitrogen sources. In period IV, the cycle length was 12 h and the feeding consisted of a short and single pulse of carbon added at the beginning of the cycle. Details concerning cycle configurations can be consulted in Fig. SI.1 and Fig. SI.2.

2.3. Batch experiments

Batch experiments were set up to evaluate the effect of the amount of carbon source added during the feast phase per unit of time and volume of the bioreactor (carbon influx, range between 0.97 and 10.62 Cmmol/(L·h)), over storage compounds accumulation.

For that purpose, a 2 L reactor was inoculated with sludge from the SBR collected at the end of the famine phase of different cycles of period III (once reached the steady-state operation). Except for the variable “carbon influx”, these batch experiments were carried out under the same conditions as those of the SBR during period III.

2.4. Sampling and analysis

For monitoring the SBR operation, the mixed liquor at the end of the cycle and the nutrient solution were periodically analyzed. Besides, to determine the evolution of the TAGs and PHAs accumulated, samples for solid-phase analysis were taken at the end of the feast phase. Regarding the SBR cycles characterized, samples were taken during the whole cycle. In the feast phase, sampling took place just before the addition of each carbon pulse (the same strategy was considered in the batch

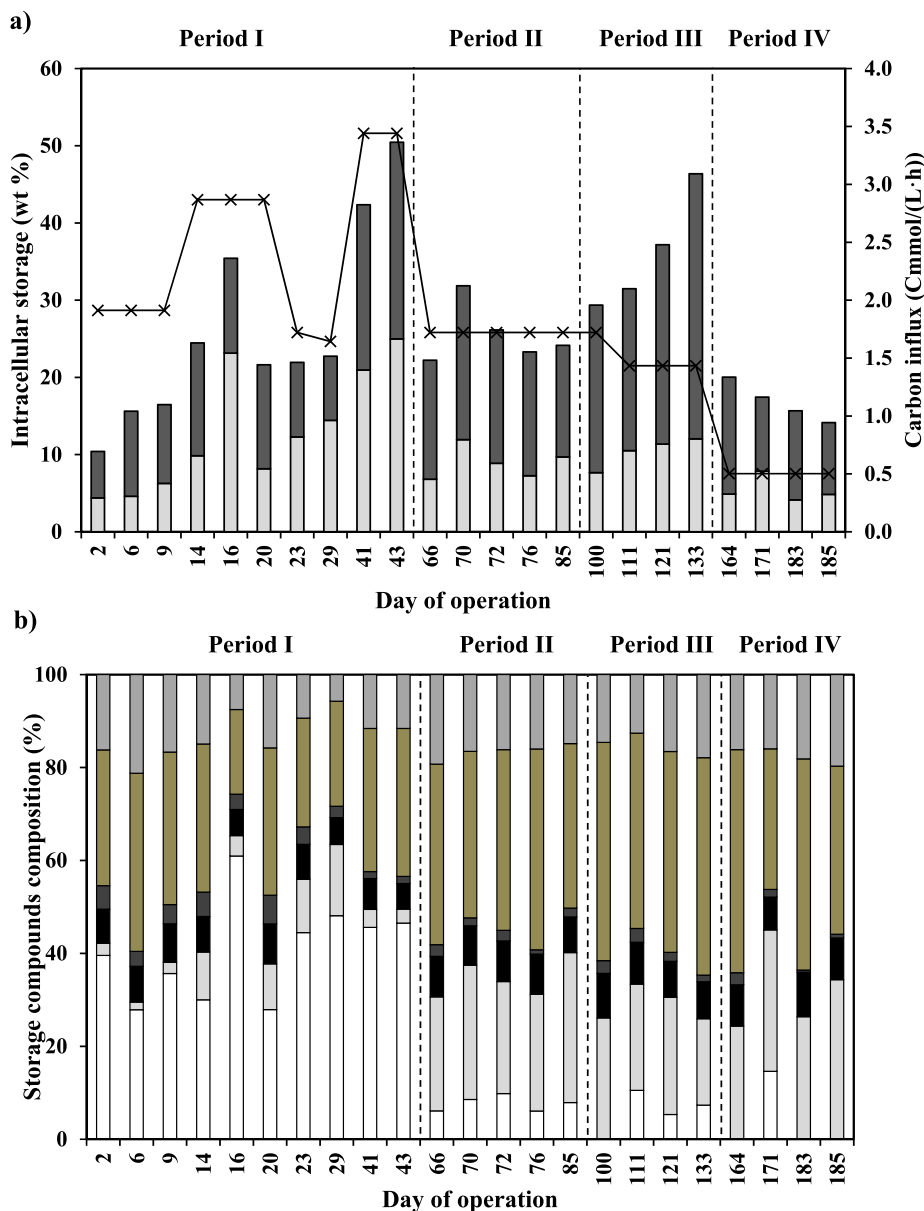


Fig. 2. (a) Maximum TAG (■) and PHA (■) accumulated at the end of the feast phase in different SBR cycles and carbon influx (×). (b) Composition of the intracellular compounds accumulated: PHB (□), PHV (□), Palmitic (■), Stearic (■), Oleic (■), Linoleic (■).

assays).

Temperature and DO concentrations were measured online by a portable multimeter (HQ40d, Hach-Lange, USA), and the pH-value was determined by a pH and Ion-Meter (GLP 22 Crison, Spain). Total suspended solids (TSS), volatile suspended solids (VSS), total chemical oxygen demand (t COD), and soluble chemical oxygen demand (s COD) were analyzed according to the standard methods for the examination of water and wastewater (Yamaguchi et al., 2016). Ions were measured by ion chromatography 861 Advanced Compact IC Metrohm, Switzerland), and total organic carbon, inorganic carbon, and total nitrogen (TOC, IC, and TN, respectively) by catalytic combustion (TOC-L analyzer with the TNM-module, TOC-5000 Shimadzu, Japan). COD_s , NH_4^+ ions, TOC, IC, and TN were measured in the soluble fraction after both centrifugation (Centrifuge 5430 Eppendorf, USA) and filtration (0.45 μ m pore size, cellulose-ester membrane, Advantec, Japan) of the raw samples. For the substrate characterization, its elemental composition was determined in an elemental analyzer (FlashEA 1112 Thermo Scientific, USA), and its fatty acids profile by gas chromatography according to ISO 12966-2:2011 (4.2) fast method and ISO 12966-4:2015.

To determine the amount and composition of the intracellular compounds accumulated, TAGs and PHAs were determined by gas chromatography (HP innovax column equipped with a FID, Agilent, USA) following the method described by Smolders et al. (1994). For that purpose, fresh biomass samples were taken, centrifuged (Centrifuge 5430 Eppendorf, USA), frozen, and lyophilized to obtain a solid phase. The stored compounds were quantified by using commercial calibration standards of TAGs (palmitic-, stearic-, oleic, and linoleic-acids) and PHAs (copolymer containing 88% 3-hydroxybutyrate (3HB) and 12% 3-hydroxyvalerate (3HV)) (Sigma Aldrich, USA).

Analyses were carried out in duplicate for each sample, except those concerning the waste substrate characterization, which were performed in triplicate.

2.5. Calculations

The storage compounds content of the biomass samples was expressed in dry weight (wt %) on a mass basis as a percentage of the measured VSS. Active biomass (X) concentration was estimated by the

Table 2

Intracellular accumulation, kinetic parameters and yields determined in: (a) 12, 18 and 24 h cycles monitored in the SBR; (b) 12 h batch assays performed during period III to test the influence of the carbon influx.

Parameter	Period I (day 43)	Period II (day 72)	Period III (day 133)
C influx (Cmmol/(L·h))	3.42	1.71	1.45
Intracellular storage (wt %)	50.24 ± 0.44	30.75 ± 1.67	45.31 ± 2.18
HB:HV:PAL:STE:OL:LIN	46:3:6:1:32:12	9:26:9:2:37:17	8:17:8:1:48:18
q_{TAG} (Cmmol _{TAG} /Cmmol _X ·h)	0.073	0.020	0.083
q_{PHA} (Cmmol _{PHA} /Cmmol _X ·h)	0.088	0.012	0.016
q_{BIOP} (Cmmol _{PHA} /Cmmol _X ·h)	0.162	0.032	0.099
q_N (Cmmol _N /Cmmol _X ·h)	- 0.001/- 0.012	-0.006/-0.010	- 0.001/- 0.005
q_S (Cmmol _S /Cmmol _X ·h)	- 0.458	- 0.069	- 0.164
q_X (Cmmol _S /Cmmol _S ·h)	0.002/0.003	0.006/0.064	0.008/0.0105
Y_{TAG} (Cmmol _{TAG} /Cmmol _S)	0.192	0.186	0.489
Y_{PHA} (Cmmol _{PHA} /Cmmol _S)	0.231	0.113	0.097
Y_{BIOP} (Cmmol _{PHA} /Cmmol _S)	0.423	0.299	0.586
Y_X (Cmmol _X /Cmmol _S)	0.023/0.049	0.425/0.390	0.086/0.478

Parameter	Assay				
	A	B*	C	D	E
C influx (Cmmol/(L·h))	0.97	1.45	3.41	7.12	10.62
Intracellular storage (wt %) **	47.05 ± 2.89	45.31 ± 2.18	57.88 ± 1.50	59.21 ± 1.49	54.92 ± 0.065
HB:HV:PAL STE:OLE:LIN **	16:16:8:2:45:15	8:17:8:1:48:18	7:11:9:2:52:19	5:7:11:3:55:20	9:9:11:2:51:20:
q_{BIOP} (Cmmol _{PHA} /Cmmol _X ·h)	0.087	0.099	0.161	0.257	0.222
q_N (Cmmol _N /Cmmol _X ·h)	1.789·10 ⁻⁵	4.813·10 ⁻⁴	5.387·10 ⁻³	1.072·10 ⁻⁴	3.676·10 ⁻⁵
q_S (Cmmol _S /Cmmol _X ·h)	0.161	0.164	0.0446	0.865	1.193
q_X (Cmmol _X /Cmmol _S ·h)	0.035	0.008	0.003	0.004	0.008
Y_{BIOP} (Cmmol _{PHA} /Cmmol _S)	0.846	0.586	0.402	0.301	0.274
Y_X (Cmmol _X /Cmmol _S)	0.340	0.086	0.080	0.055	0.120

* Data from SBR cycle monitored on day 133.

** Results obtained after 12 h. Biopolymer (BIOP), carbon (C), linoleic (LIN), nitrogen (N), palmitic (PAL), polyhydroxyalkanoates (PHA), hydroxybutyrate (HB), hydroxyvalerate (HV), maximum specific production rate (q), stearic (STE), substrate (S), triacylglyceride (TAG), oleic (OL), active biomass (X), maximum production yield (Y).

difference between the mass of VSS and that of the sum of biopolymers accumulated (BIOP = TAGs + PHAs), and it was considered CH_{1.8}O_{0.5}N_{0.2} as its monomer formula (Argiz et al., 2021a, 2021b). Maximum specific consumption of carbon substrate and nitrogen (-q_S, -q_N, respectively) and maximum specific production rates of TAG, PHA, and biomass (q_{TAG}, q_{PHA}, q_X, respectively) were determined from the maximum slopes of the curves describing the evolution of the different parameters over time. These were expressed as Cmmol/(Cmmol_X·h) except for q_X, which was referred to the substrate (S) and defined as Cmmol/(Cmmol_S·h). Production yields (Y, expressed as Cmmol/Cmmol_S) were calculated by dividing the production rates by the substrate consumption rates.

2.6. Microbial analysis

Samples for microbial analysis were collected from the SBR throughout the different operational periods: days 0, 15, 38, 43, and 51 (period I); 59, 72, 87 (period II); 107, 119, 129 (period III) 171, 183 and 188 (period IV). These were centrifuged (Centrifuge 54417 R, Eppendorf, USA) (20,817 rcf, 1 min), supernatants were discarded, and the resulting biomass was frozen and kept at -20 °C. Total deoxyribonucleic acid (DNA) content was extracted by the FastDNA SPIN Kit and the FastPrep 24-Instrument (MP Biomedicals, Germany). DNA extracts were subjected to qPCR and Illumina sequencing for both bacterial 16 S rRNA and fungal 18 S rRNA genes.

Total bacterial and fungal quantifications were made using the primers 341 F/534 R (Muyzer et al., 1993) and FungiQuantF/FungiQuantR (Liu et al., 2012), respectively. Illumina sequencing was performed using the primers Pro341 F and Pro805 R (Takahashi et al., 2014) and FungiQuantF and FungiQuantR for Bacteria and Fungi, respectively. Default settings were used for the bioinformatics process through Mothur V1.44.3. Operational taxonomic units (OTUs) were assigned at the 97% cut-off level. Singleton OTUs with a relative abundance (RA) > 0.0001% were removed for later analysis. Finally, taxonomic classifications were made by using the 16 S and 18 S

ribosomal database from the National Center for Biotechnology Information (U.S.) using the blast tool of the Geneious Prime v.2019 software (Geneious, U.S.). 16 S rRNA and 18 S rRNA sequences retrieved in this research work were deposited in GeneBank under the accession number SUB10566052.

3. Results and discussion

3.1. Single-unit process for simultaneous culture enrichment and storage compounds accumulation

During Period I (start-up – day 57) it was evaluated if culture enrichment and intracellular storage maximization could occur simultaneously in a single SBR fed with non-pretreated waste fish oil.

Initially, in the start-up (days 0–17), a single substrate pulse was fed at the beginning of the feast phase to promote culture acclimation to such a complex and hydrophobic substrate. Once observed the typical F/F profile (day 3, 6 operational cycles), the carbon influx was increased (from 1.9 to 2.9 Cmmol/(L·h) before nitrogen supply). During this start-up stage, it was observed a continuous improvement in the system storage capacity (Fig. 2a). Thus, between days 2 and 16, intracellular accumulation at the end of the feast phase increased from 10.41 ± 0.07 wt % to 35.42 ± 0.20 wt %, which indicated that the culture was being enriched in storing microorganisms, mainly in TAG-producers (the TAG: PHA ratio shifted from 42:58 to 65:35). Besides, the feast/cycle length ratio was maintained at 0.19 ± 0.07, which also evidenced the enrichment of the culture since values lower than 0.25 are associated with mixed cultures with a high storage ability rather than with a growth response (Dionisi et al., 2005).

To maintain the system pH-value among neutrality (Table 1) and allow for both substrate bioavailability and intracellular TAGs and PHAs storage (Argiz et al., 2021a, 2021b), NaHCO₃ buffer concentration in the nutrient's solution needed to be progressively adjusted (Fig. SI.3.a). The same occurred with nitrogen supply (Fig. SI.3. b), NH₄Cl concentration in the nutrient's solution was gradually reduced to the minimum

amount required for growth to assure nitrogen absence during the feast phase and avoid the development of non-storing populations when the extracellular substrate was available (Lorini et al., 2020).

After day 20, waste fish oil was started to be supplied in pulses. Pulse's frequency, and hence the carbon influx during the feast phase were adjusted according to DO profiles and gradually increased until day 36 reaching a maximum of 3.44 Cmmol/(L·h) during the feast phase (Table 1). Despite a sharp reduction of the system storage capacity immediately after shifting the feeding strategy (Fig. 2a), on day 43 a maximum intracellular accumulation of 50.45 ± 0.22 wt % (TAG:PHA ratio 49.5:50.5) was observed after 6 h of feast. At this moment, maximum production rates of 0.073 Cmmol_{TAG}/(Cmmol_S·h) and 0.088 Cmmol_{PHA}/(Cmmol_S·h) with a substrate uptake rate of -0.458 Cmmol_S/(Cmmol_X·h) were observed, and yields of 0.192 Cmmol_{TAG}/Cmmol_S, and 0.231 Cmmol_{PHA}/Cmmol_S were obtained resulting in a total yield of 0.423 Cmmol_{BIOP}/Cmmol_S (Table 2a).

Regarding TAGs production using MMC, Tamis et al. (2015) demonstrated the possibility of storing TAGs from vegetable oil without the need for substrate pretreatment reaching a maximum intracellular accumulation of 54.00 wt %. Also, in a previous operation (Argiz et al., 2021a, 2021b), in which the same lipid-rich substrate was valorized for the obtaining of high-value storage compounds using two units (PRETEN/PRENACC, Fig. 1b), 12 h of SBR cycle operation plus almost 30 h of FBR operation were needed to reach 3.33 wt % TAGs and 82.30 wt % PHAs (1.8 g VSS/L, 0.45 g X/L) when PHAs were the main storage compound. When TAGs storage was preferred, 12 h of SBR cycle operation plus 27 additional hours in the FBR were required to accumulate 39.55 wt % TAGs and 5.8 wt % PHAs (2.1 g VSS/L, 1.1 g X/L). Therefore, total maximum productions of 0.88 and 0.67 g BIOP/(L·d) were reached respectively, whereas in the present study with the single-unit system, despite the lower biomass concentration (0.48 g VSS/L, 0.22 g X/L) a maximum of 1.21 g BIOP/(L·d) was obtained. When comparing each storage compound independently, TAG production was slightly higher in the single-unit system (0.59 vs 0.61 g/(L·d)) and PHA storage was almost 30% lower (0.85 vs. 0.59 g/(L·d)).

Therefore, the proposed simplified and compact system (PRE-TENACC) appears as a competitive alternative since, with a lower maximum intracellular accumulation, it is possible to obtain a higher specific daily production. Nonetheless, following the results obtained, increasing the biomass concentration in the system appears as one of the main aspects on which future process optimization should be focused. In this context, it could be considered the possibility of increasing the cycle length, but without compromising the system productivity. Thus, on the one hand, lengthening the feast phase would allow for applying higher carbon influxes that are expected to increase biomass production. On the other hand, lengthening the famine phase would allow for longer periods of internal carbon use for growth in the famine phase offering a more successful strategy for survival in conditions of external carbon starvation.

3.2. Effect of cycle length and its configuration

In this section, shifts in the SBR cycle configuration were explored to evaluate the effect of feast and famine phases length over a process in which culture enrichment and storage compounds accumulation were coupled in the same unit.

In period II (18 h cycle), the feast phase length was increased from 6 to 12 h whereas the famine phase was maintained at 6 h. The amount of substrate added during the feast phase was the same as the optimum of period I (206 Cmmol/cycle) but pulses frequency was reduced by half and consequently, the carbon influx during the feast phase decreased from 3.44 to 1.72 Cmmol/(L·h). The C/N ratio was maintained at similar values as those of period I (Table 1).

During period II, it was observed that carbon and nitrogen uptake rates during the feast and famine phases, respectively, decreased in comparison with period I (Table 2a) not allowing for their complete

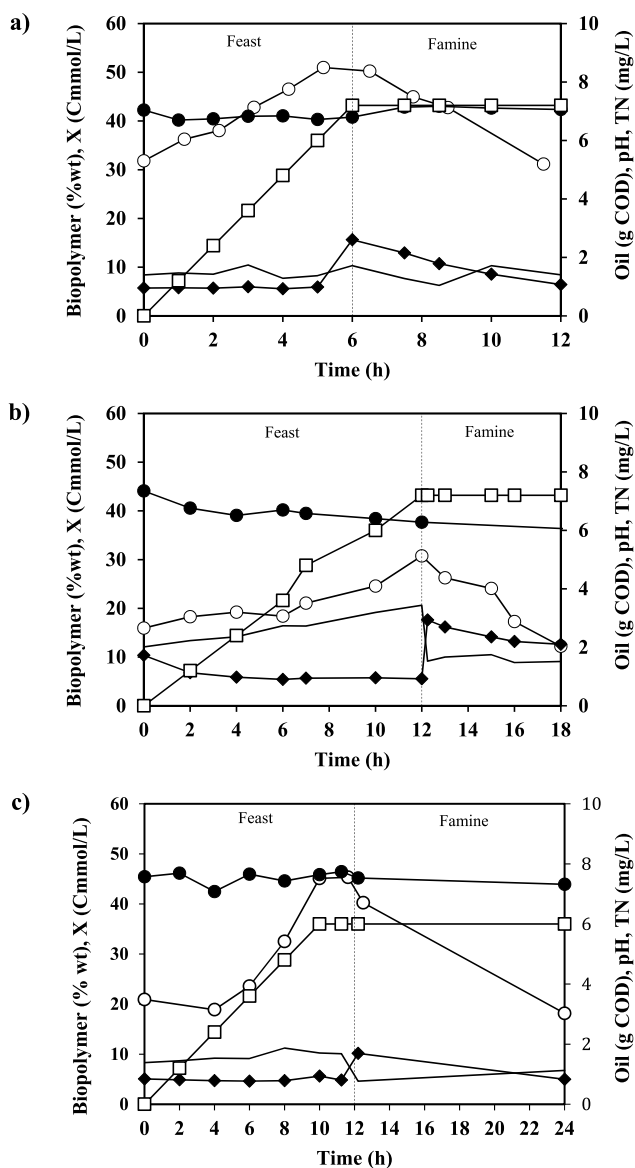


Fig. 3. Complete 12, 18 and 24 hours SBR cycles characterization. (a) Period I, day 43; (b) period II, day 72; (c) period III, day 133. pH (●), X (—), TN (◆), biopolymers as a sum of TAG + PHA (○), cumulative waste fish oil added (■).

depletion (Fig. 3b). Therefore, nitrogen was not absent during the feast phase of the subsequent cycles and an extracellular carbon source was available during the famine, allowing for non-storing populations development since both carbon and nitrogen sources were present during the whole SBR cycle. As a result, it was observed a reduction in the system storage capacity. For example, between days 43 (period I) and 72 (period II), maximum intracellular storage decreased from 50.24 ± 0.44 to 30.75 ± 1.67 wt %, and the maximum production yield diminished from 0.429 to 0.299 Cmmol_{BIOP}/Cmmol_S. Besides, it was detected a higher negative effect over PHA than over TAG producers (Fig. 2b). This affected the hydroxybutyrate (HB) fraction to a larger extent than the hydroxyvalerate (HV) one. This agrees with the fact that TAG synthesis from hydrophobic substrates via *ex novo* pathway is a growth-associated process in which accumulation and growth occur simultaneously independently from nitrogen exhaustion in the medium (Athenaki et al., 2018). On the contrary, PHA synthesis requires a metabolic decision between ATP production or internal carbon storage;

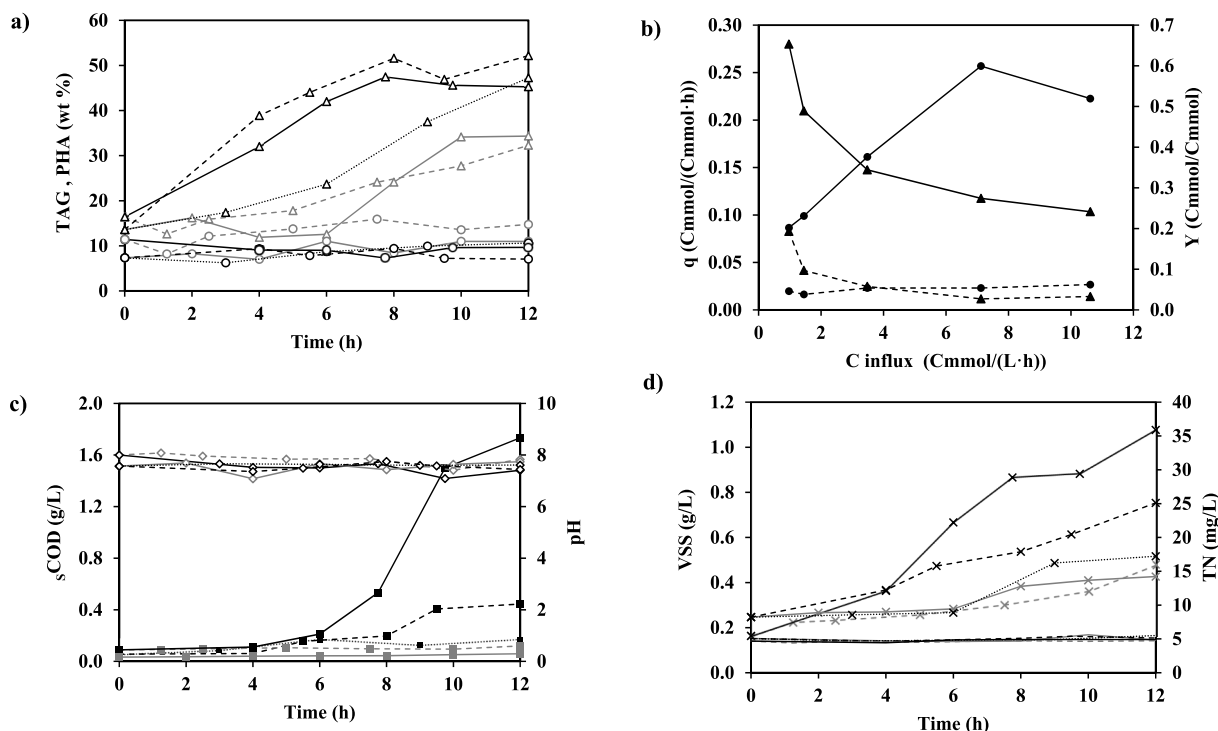


Fig. 4. Influence of the carbon influx during the feast phase over (a) intracellular TAG (Δ) and PHA (\diamond) accumulation; (b) maximum specific production rates and production yields q_{TAG} (●), q_{PHA} (●), Y_{TAG} (▲), Y_{PHA} (▲); (c) $sCOD$ (■) concentration and pH (\diamond); (d) TN (—) and VSS (×) concentrations. Tested carbon influxes in assays A – E (Cmmol/(L·h)): A 0.97 (—), B 1.45 (—), C 3.48 (---), D 7.12 (—), E 10.62 (—).

and if carbon use for growth is not nitrogen or O_2 limited, internal $[NADH]/[NAD^+]$ ratios are not expected to be high blocking PHA synthesis (Argiz et al., 2022). Besides, in this research work, it was observed that the HB fraction decreased becoming insignificant at the end of period II whereas the HV one increased (Fig. 2b). This matches with the fact that higher nitrogen concentrations lead to a higher HV fraction in PHA polymers (Alsafadi et al., 2020; Ferre-Guell and Winterburn, 2017).

In period III, to recover the system storage capacity, the cycle configuration was modified to assure carbon and nitrogen sources depletion during the feast and famine phases, respectively. For that purpose, the feast phase length was maintained at 12 h, but the carbon supply was stopped 2 h earlier (Fig. S11.c) reducing the carbon influx during the feast from 1.72 to 1.43 g Cmmol/(L·h) between periods I and II (Table 1). Besides, the famine phase length increased from 6 to 12 h and the nitrogen supply was readjusted to assure the minimum supply required for growth (Fig. S1.3. b). After switching the system configuration, it was possible to limit carbon and nitrogen availability during the feast and famine phases, respectively (Fig. 3c) leading to an increase in the culture storage capacity (Fig. 2a). Thus, this reduced the pressure towards carbon oxidation for ATP and storing populations were pushed towards intracellular compounds production (Argiz et al., 2022). For example, between days 72 (period II) and 133 (period III) intracellular storage increased from 30.75 ± 1.67 to 45.31 ± 2.18 wt % at the end of the feast phase adding a lower organic load (production yields of 0.299 and 0.586 Cmmol_{BIOP}/Cmmol_S were obtained, respectively). Also, nitrogen limitation led to a slight increase in PHA production and to the reappearance of the HB fraction, which suggests the unblocking of PHA production pathways (Fig. 2b).

The influence of the cycle length on TAG production was not previously reported. Regarding PHA production, it was explored the effect of different cycle lengths when using easy metabolizable carbon sources as a substrate and the authors agreed that although increasing the cycle length raises the PHA content of the harvested biomass, it does not ensure the selection of a culture with the highest storage capacity and productivity (Jiang et al., 2011; Marang et al., 2016; Valentino et al.,

2014). This trend in the increase of the PHA content, although not very significant, was also observed here when the cycle length was increased from 18 to 24 h between periods II and III.

3.3. Effect of the carbon influx during the feast phase

With the biomass from period III, it was studied the effect on biopolymers production of the carbon influx (from 0.97 to 10.62 Cmmol/(L·h)) during the feast phase (12 h long).

Among carbon influxes tested, maximum intracellular accumulation after 12 h was observed when 7.12 Cmmol/(L·h) was fed to the system (assay D) (Fig. 4. a; Table 2b). Specific biopolymers production was also the highest, but the production yield was considerably lower in comparison with smaller substrate influxes (Fig. 4b). Besides, about 440 mg $sCOD/L$ were measured at the end of the feast phase (Fig. 4c), leading to high extracellular substrate availability at the beginning of the famine, which would affect the MMC enrichment in a long-term operation.

It was also observed that higher carbon influxes favoured TAG storage and vice-versa. The highest intracellular storage of TAG and PHA were obtained when feeding 7.12 and 0.97 Cmmol/(L·h), respectively (Fig. 4, Table 2). This agrees with the fact that under fast rates of carbon feed, the conversion of carbon into PHA becomes rate-limiting, giving an advantage to the faster synthesis of TAG. Thus, TAG accumulation appears as a simpler process than PHA synthesis (Argiz et al., 2022).

Regarding previous studies, it was not found any research work concerning the effect of applied carbon influxes over TAG accumulation. However, the organic loading rate (OLR) effect over PHA accumulation was widely studied and, in general, it was observed that although the optimum varies, applying too high values can increase biomass production but can also extend the duration of the feast phase, reducing selective pressure and hence biopolymer production (de Oliveira et al., 2019; Dionisi et al., 2006). This fact correlates with the decreasing PHA accumulations observed when increasing the carbon influx (Fig. 4. a, Table 2b).

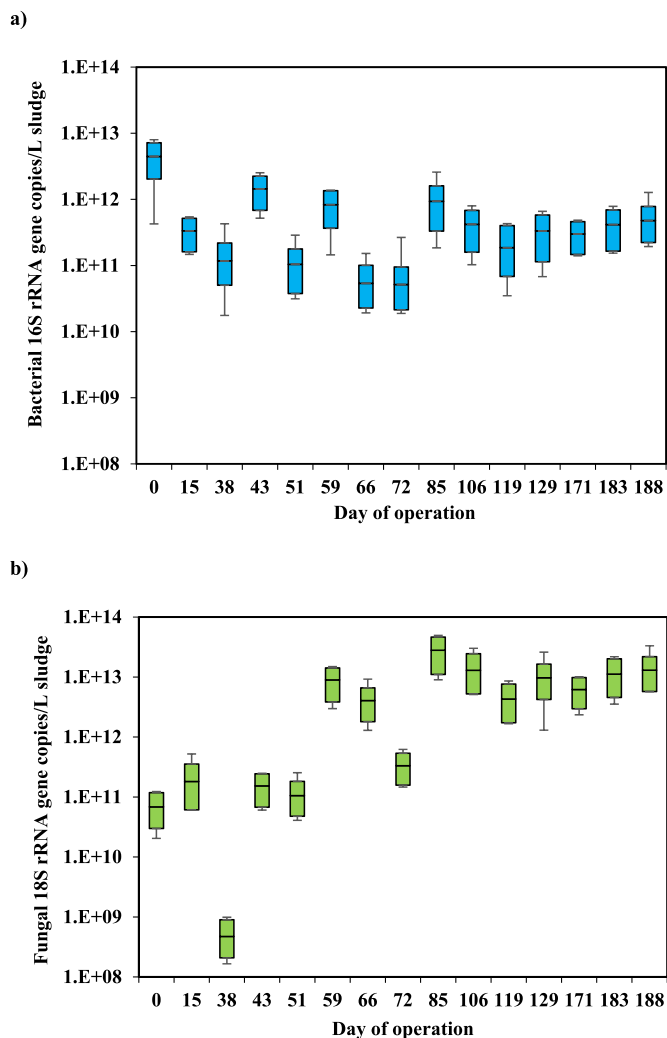


Fig. 5. Number of copies/L activated sludge for the bacterial (a) and fungal (b) 16S and 18S rRNA determined by quantitative PCR in the biomass samples retrieved from the SBR. According to the Kruskal-Wallis and Conover-Iman tests ($p < 0.05$), different lowercase letters indicate significant differences among periods.

3.4. Effect of the C/N ratio

It is well known that when growing on limiting concentrations of nitrogen with excess carbon (higher C/N ratios) not only TAG producers, but also PHA ones stop their replication processes and accumulate intracellularly the available external carbon (Garay et al., 2014). For this reason, although optimal C/N ratios widely vary with the culture composition and type of carbon source used, high C/N ratios are expected to favor both accumulation processes (Carsanba et al., 2018; Patel and Matsakas, 2019; Pozo et al., 2011; Wang et al., 2007). However, in this research work, in which TAG and PHA storing microorganisms coexist within the community, the C/N ratio seems to play an important selective role. It was observed a positive correlation between the increase in the C/N ratio and the increase in the TAG storage at the end of the feast phase (Fig. SL4), which was not so clear in the case of PHA accumulation.

Between periods III and IV both the carbon influx and the C/N ratio were reduced drastically (Table 1) by feeding a single and small pulse of the substrate at the beginning of the cycle. As expected, the reduction of substrate supply led to biomass washout in the system (Fig. SL3c), and intracellular storage at the end of the feast phase notably decreased (Fig. 4a). Nonetheless, TAG producers were observed to be more

affected than PHA ones. Thus, between days 133 (period III) and 185 (period IV), TAG storage at the end of the feast phase was reduced by 73% whereas PHA accumulation was reduced by less than 60%, and the TAG:PHA ratio varied from 74:26 to 66:34. This fact matches with the fact that lower carbon influxes (see section 3.3 Effect of the carbon influx during the feast phase) and higher C/N ratios (Fig. SL4) favor PHA and TAG storage, respectively.

When the carbon influx during the feast phase was reduced by half between periods I and II maintaining similar relatively high C/N ratios (Table 1), PHA producers were affected the most. For example, between days 44 (period I, 3.44 Cmmol/(L-h), 12.25 g C/g N-NH₄⁺) and 71 (period II, 1.72 Cmmol/(L-h), 11.63 g C/g N-NH₄⁺) TAG production decreased by 22% whereas PHA accumulation diminished by 52% (Fig. 4a). Therefore, despite reducing the carbon influx, maintaining a high C/N ratio led to a lower decrease of the system TAG than PHA storage ability.

When the C/N ratio was increased but reducing the carbon influx (periods II vs III, Table 1) while PHA production was almost maintained, TAG storage increased by 44% between days 71 (period II, 1.72 Cmmol/(L-h) g COD/L-h, 12.25 g C/g N-NH₄⁺) and 133 (period III, 1.43 Cmmol/(L-h), 18.58 g C/g N-NH₄⁺) (Fig. 4a). This fact evidences the positive effect of higher C/N ratios over TAG storage and suggests that the selective pressure exerted by this parameter is even stronger than the one caused by the carbon influx.

In contrast to the observed in this research work, previous studies concerning TAG accumulation from hydrophobic carbon sources showed that the effect of the C/N ratio on microbial growth and TAG storage was not observed to be such important as this is a growth-associated process (Patel et al., 2019). However, regarding PHA, although optimum values were observed to widely vary, authors agreed that high C/N ratios clearly favoured PHA production (Sánchez Valencia et al., 2021; Silva et al., 2021; Wang et al., 2007). Therefore, the coexistence of TAG and PHA producers within the community may play a role in the effect of the C/N ratio over preferential TAG or PHA storage.

3.5. Microbial community analysis

3.5.1. Bacterial and fungal abundance

Total abundances ranged from 4.23×10^{10} to 2.49×10^{12} bacterial 16 S rRNA gene copies/L of sludge and 3.18×10^{12} to 1.58×10^{13} fungal 18 S rRNA gene copies/L of sludge (Fig. 5). Although both populations showed variances in their magnitudes, the abundance of Fungi oscillated up to 5 orders. Significant differences were found in the total abundances of the fungal populations throughout the SBR operation (the highest in periods III and IV, and the lowest in the inoculum and period I). Regarding Bacteria, no significant differences were detected among periods I – IV and the highest values of the 16 S rRNA gene copies were found in the inoculum. Therefore, while the different cycle configurations did not influence the total abundances of *Bacteria*, clearly increased the fungal ones.

3.5.2. Bacterial and fungal diversity

It was obtained 1,554,177 high-quality sequences for Bacteria and 2,226,145 for Fungi distributed into 1180 and 117 OTUs, respectively (Table SL3; Table SL4). As a consequence of the selection strategies implemented in the SBR, both bacterial and fungal diversity richness, determined as the OTUs' numbers, notably decreased (Table SL5). Nonetheless, the Bray-Curtis analysis (Fig. SL5) showed higher differences in the bacterial community than in the fungal one due to the overdomination of the fungal OTUF001 (*Saprochaete*) after day 51. Therefore, although both communities were selected in some way, those variations implemented in the cycle configuration among the different operational periods affected the fungal community to a larger extent.

3.5.2.1. Communities structure and storage ability. The 1180 bacterial

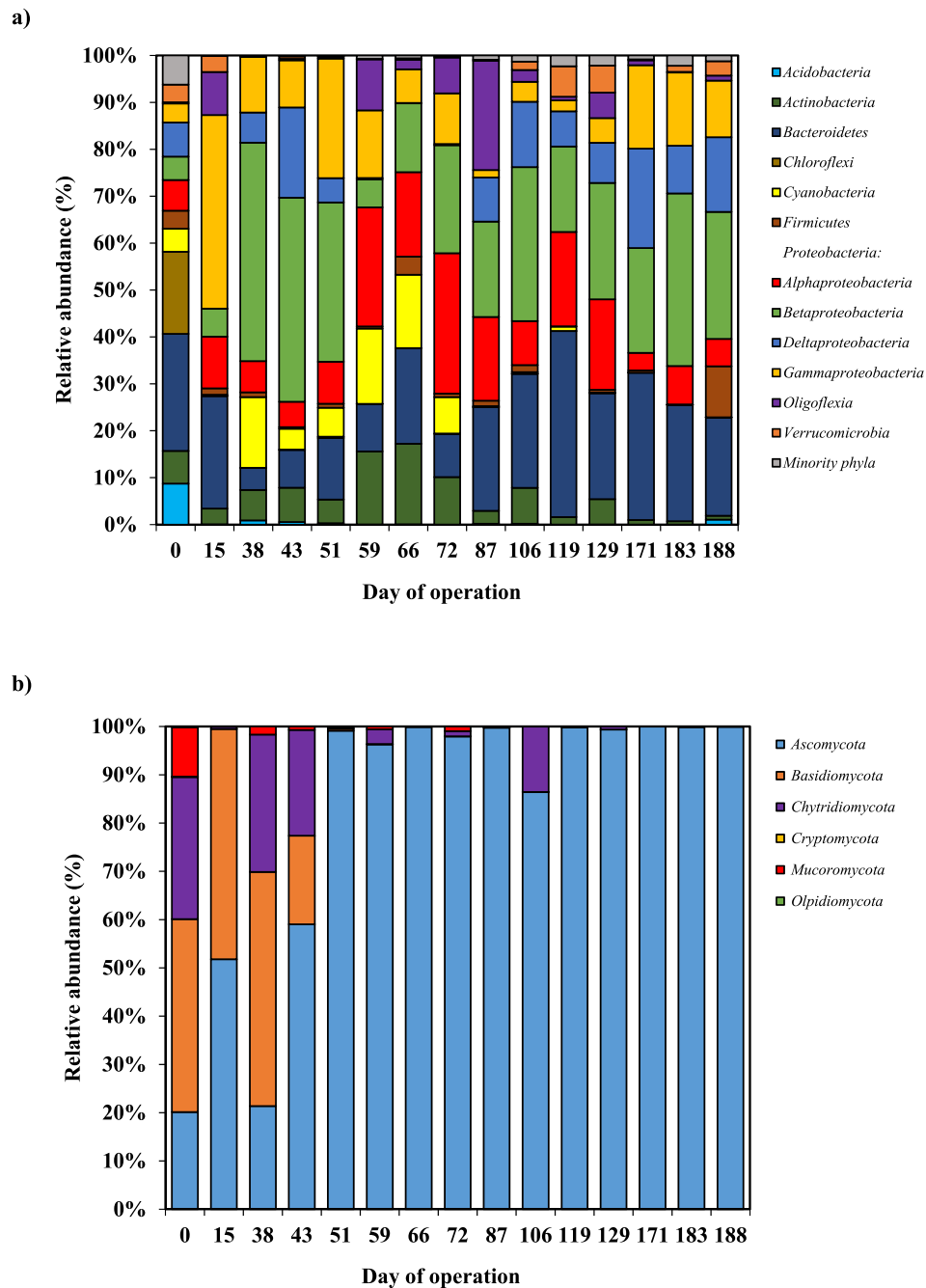


Fig. 6. RA of dominant bacterial (a) and fungal (b) OTUs (RA > 0.5 %) obtained by Illumina high-throughput sequencing in biomass samples retrieved from the SBR.

OTUs were distributed into 27 different phyla, 8 of them considered as dominant (relative abundance (RA) > 0.5%) plus a group of minority phyla. Sorted in decreasing order of average RA they were: *Proteobacteria* (62.19 ± 3.12%, subdivided in *Betaproteobacteria* (24.06 ± 2.31%), *Alphaproteobacteria* (13.08 ± 1.43%), *Gammaproteobacteria* (12.26 ± 1.82%), *Deltaproteobacteria* (8.37 ± 1.21%), and *Oligoflexia* (4.34 ± 1.12%)), *Bacteroidetes* (20.02 ± 1.67%), *Actinobacteria* (6.12 ± 0.89%), *Cyanobacteria* (4.79 ± 1.08%), *Verrucomicrobia* (1.83 ± 0.38%), *Firmicutes* (1.81 ± 0.49%), *Minority phyla* (1.27 ± 0.28%), *Chloroflexi* (1.21 ± 0.80%), and *Acidobacteria* (0.81 ± 0.39%) (Fig. 6, Table SI.6).

At the OTU level, there were 24 bacterial major OTUs (average RAs > 0.5%) (Fig. 7, Table SI.7): OtuB0001 (*Curvibacter*, 8.69 ± 2.83%), OtuB0002 (*Pseudacidovorax*, 7.35 ± 1.39%), OtuB0003 (*Kofleria*, 4.91 ± 1.21%), OtuB0004 (*Gordonia*, 4.90 ± 0.84%), OtuB0005 (*Pseudoxanthobacter*, 4.27 ± 1.14%), OtuB0006 (*Calothrix*, 3.76 ± 1.01%),

OtuB0007 (*Acinetobacter*, 2.98 ± 0.84%), OtuB0008 (*Epilithonimonas*, 2.89 ± 0.77%), OtuB0009 (*Thalassotalea*, 2.57 ± 0.68%), OtuB0010 (*Flectobacillus*, 2.44 ± 0.59%), OtuB0011 (*Runella*, 2.12 ± 0.43%), OtuB0012 (*Aquabacterium*, 2.03 ± 0.70%), OtuB0013 (*Labilithrix*, 2.03 ± 0.91%), OtuB0014 (*Pseudomonas*, 2.02 ± 0.86%), OtuB0015 (*Oligoflexus*, 2.00 ± 0.78%), OtuB0016 (*Pedobacter*, 1.83 ± 0.69%), OtuB0017 (*Bdellovibrio*, 1.53 ± 0.57%), OtuB0018 (*Stania*, 1.33 ± 0.69%), OtuB0019 (*Herbaspirillum*, 1.33 ± 0.34%), OtuB0020 (*Glaciimonas*, 1.29 ± 0.70%), OtuB0021 (*Ohtaekwangia*, 1.25 ± 0.63%), OtuB0022 (*Spirosoma*, 1.19 ± 0.51%), OtuB0023 (*Agitococcus*, 1.00 ± 0.60%), OtuB0024 (*Cloacibacterium*, 1.00 ± 0.45%), plus the hotchpotch group of the minority bacterial OTUs (34.37 ± 3.66%). Among these dominant bacteria, the following were previously described as capable of storing PHA: *Acinetobacter* (*Gammaproteobacteria*) (Anburajan et al., 2019), *Calothrix* (*Cyanobacteria*) (Kaewbai-ngam et al., 2016), *Glaciimonas*

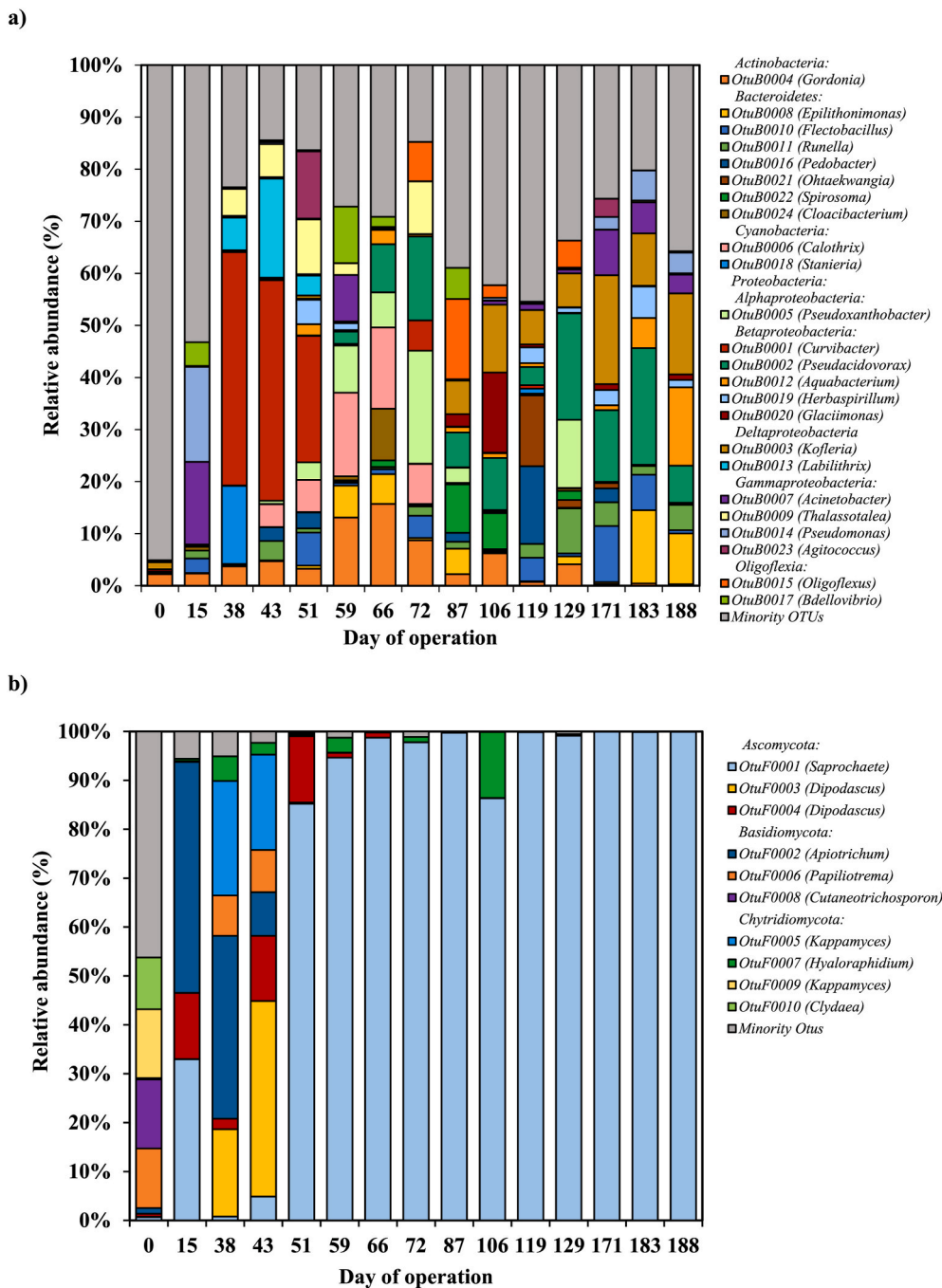


Fig. 7. RA of dominant bacterial (a) and fungal OTUs (b) (RA > 0.5 %) obtained by Illumina high-throughput sequencing in biomass samples retrieved from the SBR.

(Betaproteobacteria) (Kumar et al., 2020), *Herbaspirillum* (Betaproteobacteria) (Catalán et al., 2007), and *Pseudomonas* (Gammaproteobacteria) (Song et al., 2008). Besides, other genera have been identified in the literature as dominant in PHA-accumulating SBR fed with glycerol (*Gordonia* (Actinobacteria) (Burniol-Figols et al., 2018), and *Ohtaekwangia* (Bacteroidetes) (Wen et al., 2021)) and several low-cost substrates such as fish-canning residues (*Epilithonimonas* (Bacteroidetes) (Argiz et al., 2021a, 2021b)), urban waste (*Runella*, (Bacteroidetes) (Crognale et al., 2019)), dairy manure (*Aquabacterium*, (Betaproteobacteria) (Coats et al., 2016), paper industry waste (*Pedobacter* (Bacteroidetes) (Ferreira et al., 2016)), and lignocellulosic biomass (*Spirosoma*, (Bacteroidetes) (Yan et al., 2021)). Besides, although TAG is mainly biosynthesized by Fungi (Garay et al., 2014), some bacterial strains can also accumulate lipids. In this research, two of the dominant bacteria present in the

culture (*Gordonia* (Actinobacteria) and *Cloacibacterium* (Bacteroidetes)) were reported in the literature as capable of storing TAG (Chen et al., 2021; Gouda et al., 2008). Also, it was observed that different diazotrophic bacterial OTUs turned statistically higher when a low C influx was imposed (period IV vs. period III): OtuB0002 (*Pseudacidovorax*) (Liu et al., 2014), OtuB0007 (*Acinetobacter*) (Chaudhary et al., 2012), OtuB0014 (*Pseudomonas*) (Yan et al., 2008), and OtuB0019 (*Herbaspirillum*) (Chubatsu et al., 2012). Results match with the fact that while higher carbon availabilities favor those microorganisms capable of metabolizing lipids faster (TAG producers), lower carbon influxes may be a selective advantage for PHA producers (see section 3.3. Effect of the carbon influx during the feast phase).

The 117 fungal OTUs belonged to 5 different phyla, which sorted in decreased order of RA were: Ascomycota (82.05 ± 5.24%),

Basidiomycota (10.35 ± 3.38%), Chytridiomycota (6.62 ± 1.97%), Mucoromycota (0.96 ± 0.47%), Cryptomycota (0.01 ± 0.01%), and Olpidiomycota (0.01 ± 0.01%) (Fig. 6, Table SI.8). Out of the 117 fungal OTUs, 10 were considered as major (Fig. 7, Table SI.9): OtuF0001 (*Saprochaete*, 73.36 ± 7.28%), OtuF0002 (*Apiotrichum*, 6.34 ± 2.67%), OtuF0003 (*Dipodascus*, 3.88 ± 1.97%), OtuF0004 (*Dipodascus*, 3.02 ± 0.98%), OtuF0005 (*Kappamyces*, 2.88 ± 1.36%), OtuF0006 (*Papiliotrema*, 1.95 ± 0.73%), OtuF0007 (*Hyaloraphidium*, 1.77 ± 0.64%), OtuF0008 (*Cutaneotrichosporon*, 0.95 ± 0.65%), OtuF0009 (*Kappamyces*, 0.94 ± 0.65%), OtuF0010 (*Clydaea*, 0.71 ± 0.49%), and the group of minority fungal OTUs (4.20 ± 2.11%). Among these dominant OTUs, the following genera have been previously described in the literature as TAG producers: *Apiotrichum* (Basidiomycota) (Qian et al., 2021), *Cutaneotrichosporon* (Basidiomycota) (Awad et al., 2019), *Dipodascus* (Ascomycota) (Smith et al., 2003), and *Papiliotrema* (Basidiomycota) (Moreira Vieira et al., 2020). Also, some species of *Saprochaete* (Ascomycota) were formerly taxonomically classified within the genus *Geotrichum*, a well-known TAG-accumulation yeast (Diwan and Gupta, 2020). Although there are no data available reporting its TAG production, the high intracellular TAG accumulations obtained once this OTU turned dominant (Fig. 7, Table 2) suggests that *Saprochaete* presents a high TAG-storage ability.

There were several statistical differences for the RAs of the dominant bacterial and fungal phyla among periods I – IV (Table SI.6; Table SI.8), which confirms that the operational conditions applied in the SBR resulted in a significant selection of the microbial communities.

The Spearman correlation test showed that the total abundance of Bacteria or Fungi could not be correlated with PHA or TAG storage (Table SI.10). Also, it demonstrated that only OtuF0003 (*Dipodascus*), OtuF0006 (*Papiliotrema*), and OtuF0007 (*Hyaloraphidium*) were positive and significantly correlated with TAG-accumulation. No positive correlations were found between PHA accumulation and the RAs of any of the dominant OTUs. Besides, only OtuB0008 (*Epilithonimonas*) and OtuB0012 (*Aquabacterium*) showed negative correlations with PHA and TAG accumulation, respectively. Therefore, PHA and TAG storage levels were poorly associated with the increased RAs of specific OTUs, suggesting a functional redundancy in both TAG and PHA biosynthesis pathways. Therefore, further research is necessary to assess the expression of the key genes concerning TAG and PHA synthesis pathways of the dominant OTUs here described.

3.5.2.2. Interactions between communities. The co-occurrence network constructed to evaluate the interactions between bacterial and fungal communities (Fig. SI.6) consisted of 35 nodes (OtuB0018 (*Stantieria*) did not present any significant correlation with the remaining dominant OTUs) and 284 edges representing 22.54% of the potential correlations. The number of significant interactions was 92 between dominant bacterial OTUs (32.40% of the total interaction), 72 between dominant fungal OTUs (25.35%), and 120 between bacterial and fungal OTUs (42.35%). Therefore, the network showed abundant synergistic interrelationships between bacterial and fungal communities, which favor the adaptation to environmental changes (Layeghifard et al., 2017) like the different pressures imposed when varying the SBR cycle configuration. Except for OtuB0003 (*Kofleria*, 5 positives, and 9 negatives), all the OTUs with a high level of syntrophic interactions have potential accumulative roles being pivotal players in maintaining the structure of the storing community (Qian et al., 2019) (OtuF0002 (*Apiotrichum*, 11 positives, and 7 negatives), OtuF0001 (*Saprochaete*, 8 positive and 9 negatives), OtuF0006 (*Papiliotrema*, 8 positives, and 8 negatives), minority fungal Otus (7 positives and 8 negatives), OtuB0021 (*Ohtaekwangia*, 6 positives, and 8 negatives), and OtuF0004 (*Dipodascus*, 8 positives, and 6 negatives).

4. Conclusions

This research work demonstrated feasibility in the production of value-added storage compounds from a non-pretreated lipid-rich waste stream using a single-unit process (PRETENACC) in which pretreatment, enrichment, and accumulation stages were coupled in a unique SBR. This study led the way for a competitive lipid-rich effluents valorization in the frame of a circular economy model. PRETENACC appears as a simplified and more economically feasible alternative that can be used for the transformation of high-loaded lipid-rich streams, like those generated in several food industries, into valuable compounds (TAGs and PHAs). Maximum intracellular storage of 51 wt % (TAG:PHA ratio of 50:51) and a production yield of 0.423 Cmmol_{BIOP}/Cmmol_S were reached after only 6 h of feast phase when the system was operated under 12 h cycles resulting in a higher daily biopolymer production than the obtained in a previously operated two-stage process when using the same substrate. Also, certain parameters were observed to play an important role in the single-unit process performance: feast and famine phases length, the carbon influx, and the C/N ratio. Regarding the microbial community structure, while variations in the operational conditions were observed to modulate the fungal one, the bacterial community was not found to be affected.

Therefore, given the great potential of PRETENACC process, the next step is to increase the degree of maturity of the biotechnology by moving on to pilot-scale to validate its performance and evaluate its technical, economic, and environmental feasibility.

Declaration of competing interest

The authors declare that they have no known competing financial interests or personal relationships that could have appeared to influence the work reported in this paper.

Acknowledgments

This research was supported by the Spanish Government (AEI, Spain) through the TREASURE project [CTQ 2017-83225-C2-1-R]. Lucía Argiz is a Xunta de Galicia fellow [ED 484A-2019/083] (GAIN, Galicia, Spain), grant is co-funded by the operative program FSE Galicia 2014–2020. The authors belong to the Galician Competitive Research Group GRC ED431C 2017/29. All these programs are co-funded by the FEDER (EU).

Appendix A. Supplementary data

Supplementary data to this article can be found online at <https://doi.org/10.1016/j.jenvman.2022.115433>.

References

- Albuquerque, M.G.E., Eiroa, M., Torres, C., Nunes, B.R., Reis, M.A.M., 2007. Strategies for the development of a side stream process for polyhydroxyalkanoate (PHA) production from sugar cane molasses. *J. Biotechnol.* 130, 411–421. <https://doi.org/10.1016/j.jbiotec.2007.05.011>.
- Alsafadi, D., Al-Mashaqbeh, O., Mansour, A., Alsaad, M., 2020. Optimization of nitrogen source supply for enhanced biosynthesis and quality of poly(3-hydroxybutyrate-co-3-hydroxyvalerate) by extremely halophilic archaeon *Haloflex mediterranei*. *Microbiologyopen* 9, 1–9. <https://doi.org/10.1002/mbo3.1055>.
- Alvarez, Héctor M., Roxana, A., Silva, M.H., Hernández, Martín A., María, A., Villalba, S., 2013. Metabolism of triacylglycerols in *Rhodococcus* species: insights from physiology and molecular genetics. *J. Mol. Biochem.* 2, 69–78.
- Alvarez, H.M., Steinbüchel, A., 2002. Triacylglycerols in prokaryotic microorganisms. *Appl. Microbiol. Biotechnol.* 60, 367–376. <https://doi.org/10.1007/s00253-002-1135-0>.
- Anburajan, P., Naresh Kumar, A., Sabapathy, P.C., Kim, G.B., Cayetano, R.D., Yoon, J.J., Kumar, G., Kim, S.H., 2019. Polyhydroxy butyrate production by *Acinetobacter junii* BP25, *Aeromonas hydrophila* ATCC 7966, and their co-culture using a feast and famine strategy. *Bioresour. Technol.* 293, 122062. <https://doi.org/10.1016/j.biortech.2019.122062>.
- Argiz, L., Correa-galeote, D., Val, Á., Mosquera-corrall, A., González-cabaleiro, R., 2022. Science of the Total Environment Valorization of lipid-rich wastewaters: a theoretical analysis to tackle the competition between polyhydroxyalkanoate and

- triacylglyceride-storing populations. *Sci. Total Environ.* 807, 150761 <https://doi.org/10.1016/j.scitotenv.2021.150761>.
- Argiz, Lucía, Gonzalez-Cabaleiro, R., Correa-Galeote, D., Val del Rio, A., Mosquera-Corral, A., 2021a. Open-culture biotechnological process for triacylglycerides and polyhydroxyalkanoates recovery from industrial waste fish oil under saline conditions. *Separ. Purif. Technol.* 270, 118805 <https://doi.org/10.1016/j.seppur.2021.118805>.
- Argiz, Lucía, González Cabaleiro, R., Val del Río, Á., González-López, J., Mosquera-Corral, A., 2021b. A novel strategy for triacylglycerides and polyhydroxyalkanoates production using waste lipids. *Sci. Total Environ.* 763 <https://doi.org/10.1016/j.scitotenv.2020.142944>.
- Athenaki, M., Gardeli, C., Diamantopoulou, P., Tchakouteu, S.S., Sarris, D., Philippoussis, A., Papanikolaou, S., 2018. Lipids from yeasts and fungi: physiology, production and analytical considerations. *J. Appl. Microbiol.* 124, 336–367. <https://doi.org/10.1111/jam.13633>.
- Awad, D., Bohnen, F., Mehlmer, N., Brueck, T., 2019. Multi-factorial-guided media optimization for enhanced biomass and lipid formation by the oleaginous yeast *Cutaneotrichosporon oleaginosus*. *Front. Bioeng. Biotechnol.* 7 <https://doi.org/10.3389/fbioe.2019.00054>.
- Bharathiraja, B., Sridharan, S., Sowmya, V., Yuvaraj, D., Praveenkumar, R., 2017. Microbial oil – a plausible alternate resource for food and fuel application. *Bioresour. Technol.* 233, 423–432. <https://doi.org/10.1016/j.biortech.2017.03.006>.
- Burniol-Figols, A., Varrone, C., Daugaard, A.E., Le, S.B., Skiadas, I.V., Gavala, H.N., 2018. Polyhydroxyalkanoates (PHA) production from fermented crude glycerol: study on the conversion of 1,3-propanediol to PHA in mixed microbial consortia. *Water Res.* 128, 255–266. <https://doi.org/10.1016/j.watres.2017.10.046>.
- Campanari, S., Augelletti, F., Rossetti, S., Sciubba, F., Villano, M., Majone, M., 2017. Enhancing a multi-stage process for olive oil mill wastewater valorization towards polyhydroxyalkanoates and biogas production. *Chem. Eng. J.* <https://doi.org/10.1016/j.cej.2017.02.094>.
- Carsanba, E., Papanikolaou, S., Erten, H., 2018. Production of oils and fats by oleaginous microorganisms with an emphasis given to the potential of the nonconventional yeast *Yarrowia lipolytica*. *Crit. Rev. Biotechnol.* 38, 1230–1243. <https://doi.org/10.1080/07388551.2018.1472065>.
- Catalán, A.L., Ferreira, F., Gill, P.R., Batista, S., 2007. Production of polyhydroxyalkanoates by *Herbaspirillum seropedicae* grown with different sole carbon sources and on lactose when engineered to express the lacZlacY genes. *Enzym. Microb. Technol.* 40, 1352–1357. <https://doi.org/10.1016/j.enzmictec.2006.10.008>.
- Chan, L.G., Cohen, J.L., Ozturk, G., Hennebel, M., Taha, A.Y., De Moura Bell, J.M.L.N., 2018. Bioconversion of cheese whey permeate into fungal oil by *Mucor circinelloides*. *J. Biol. Eng.* 12, 1–14. <https://doi.org/10.1186/s13036-018-0116-5>.
- Chaudhary, H.J., Peng, G., Hu, M., He, Y., Yang, L., Luo, Y., Tan, Z., 2012. Genetic diversity of endophytic diazotrophs of the Wild Rice, *Oryza alta* and identification of the new diazotroph, acinetobacter *oryzae* sp. nov. *Microb. Ecol.* 63, 813–821. <https://doi.org/10.1007/s00248-011-9978-5>.
- Chen, H., Zou, M., Zhou, Y., Zeng, L., Yang, X., 2021. Monitoring the nitrous oxide emissions and biological nutrient removal from wastewater treatment: impact of perfluorooctanoic acid. *J. Hazard Mater.* 402, 123469 <https://doi.org/10.1016/j.jhazmat.2020.123469>.
- Chubatsu, L.S., Monteiro, R.A., de Souza, E.M., de Oliveira, M.A.S., Yates, M.G., Wassem, R., Bonatto, A.C., Huergo, L.F., Steffens, M.B.R., Rigo, L.U., Pedrosa, F. de O., 2012. Nitrogen fixation control in *Herbaspirillum seropedicae*. *Plant Soil* 356, 197–207. <https://doi.org/10.1007/s11104-011-0819-6>.
- Coats, E.R., Watson, B.S., Brinkman, C.K., 2016. Polyhydroxyalkanoate synthesis by mixed microbial consortia cultured on fermented dairy manure: effect of aeration on process rates/yields and the associated microbial ecology. *Water Res.* 106, 26–40. <https://doi.org/10.1016/j.watres.2016.09.039>.
- Crognale, S., Tonanzi, B., Valentino, F., Majone, M., Rossetti, S., 2019. Microbiome dynamics and phaC synthase genes selected in a pilot plant producing polyhydroxyalkanoate from the organic fraction of urban waste. *Sci. Total Environ.* 689, 765–773. <https://doi.org/10.1016/j.scitotenv.2019.06.491>.
- de Oliveira, G.H.D., Niz, M.Y.K., Zaiat, M., Rodrigues, J.A.D., 2019. Effects of the organic loading rate on polyhydroxyalkanoate production from sugarcane stillage by mixed microbial cultures. *Appl. Biochem. Biotechnol.* 189, 1039–1055. <https://doi.org/10.1007/s12010-019-03051-9>.
- Dionisi, D., Beccari, M., Gregorio, S. Di, Majone, M., Papini, M.P., Vallini, G., 2005. Storage of biodegradable polymers by an enriched microbial community in a sequencing batch reactor operated at high organic load rate, 1318, pp. 1306–1318. <https://doi.org/10.1002/jctb.1331>.
- Dionisi, D., Majone, M., Vallini, G., Di Gregorio, S., Beccari, M., 2006. Effect of the applied organic load rate on biodegradable polymer production by mixed microbial cultures in a sequencing batch reactor. *Biotechnol. Bioeng.* 93, 76–88. <https://doi.org/10.1002/bit.20683>.
- Diwan, B., Gupta, P., 2020. A deuteromycete isolate *Geotrichum candidum* as oleaginous cell factory for medium-chain fatty acid-rich oils. *Curr. Microbiol.* 77, 3738–3749. <https://doi.org/10.1007/s00284-020-02155-4>.
- Ferre-Guell, A., Winterburn, J., 2017. Production of the copolymer poly(3-hydroxybutyrate-co-3-hydroxyvalerate) with varied composition using different nitrogen sources with *Haloflex mediterranei*. *Extremophiles* 21, 1037–1047. <https://doi.org/10.1007/s00792-017-0964-9>.
- Ferreira, A.M., Queirós, D., Gagliano, M.C., Serafim, L.S., Rossetti, S., 2016. Polyhydroxyalkanoates-accumulating bacteria isolated from activated sludge acclimatized to hardwood sulphite spent liquor. *Ann. Microbiol.* 66, 833–842. <https://doi.org/10.1007/s13213-015-1169-z>.
- Frkova, Z., Venditti, S., Herr, P., Hansen, J., 2020. Assessment of the production of biodiesel from urban wastewater-derived lipids. *Resour. Conserv. Recycl.* 162, 105044 <https://doi.org/10.1016/j.resconrec.2020.105044>.
- Garay, L.A., Boundy-Mills, K.L., German, J.B., 2014. Accumulation of high-value lipids in single-cell microorganisms: a mechanistic approach and future perspectives. *J. Agric. Food Chem.* 62, 2709–2727. <https://doi.org/10.1021/jf4042134>.
- Gobi, K., Vadivelu, V.M., 2014. Aerobic dynamic feeding as a strategy for in situ accumulation of polyhydroxyalkanoate in aerobic granules. *Bioresour. Technol.* 161, 441–445. <https://doi.org/10.1016/j.biortech.2014.03.104>.
- Gouda, M.K., Omar, S.H., Aouad, L.M., 2008. Single cell oil production by *Gordonia* sp. DG using agro-industrial wastes. *World J. Microbiol. Biotechnol.* 24, 1703–1711. <https://doi.org/10.1007/s11274-008-9664-z>.
- Herrero, O.M., Villalba, M.S., Lanfranconi, M.P., Alvarez, H.M., 2018. Rhodococcus bacteria as a promising source of oils from olive mill wastes. *World J. Microbiol. Biotechnol.* 34 <https://doi.org/10.1007/s11274-018-2499-3>, 0.
- Husain, I.A.F., Alkhatib, M.F., Jamm, M.S., Mirghani, M.E.S., Zainudin, Z. Bin, Hoda, A., 2014. Problems, control, and treatment of fat, oil, and grease (FOG): a review. *J. Oleo Sci.* 63, 747–752. <https://doi.org/10.5650/jos.ess13182>.
- Jiang, Y., Marang, L., Kleerebezem, R., Muzzer, G., Van Loosdrecht, M.C.M., 2011. Effect of temperature and cycle length on microbial competition in PHB-producing sequencing batch reactor. *ISME J.* 5, 896–907. <https://doi.org/10.1038/ismej.2010.174>.
- Kaewbai-ngam, A., Incharoenakdi, A., Monshupanee, T., 2016. Increased accumulation of polyhydroxybutyrate in divergent cyanobacteria under nutrient-deprived photoautotrophy: an efficient conversion of solar energy and carbon dioxide to polyhydroxybutyrate by *Calothrix scytonemica* TISTR 8095. *Bioresour. Technol.* 212, 342–347. <https://doi.org/10.1016/j.biortech.2016.04.035>.
- Kourmentza, C., Plácido, J., Venetsaneas, N., Burniol-Figols, A., Varrone, C., Gavala, H. N., Reis, M.A.M., 2017. Recent advances and challenges towards sustainable polyhydroxyalkanoate (PHA) production. *Bioengineering* 4, 55. <https://doi.org/10.3390/bioengineering4020055>.
- Kumar, Vijay, Thakur, V., Ambika, Kumar, Virender Kumar, R., Singh, D., 2020. Genomic insights revealed physiological diversity and industrial potential for *Glaucimonas* sp. PCH181 isolated from Satrundi glacier in Pangi-Chamba Himalaya. *Genomics* 112, 637–646. <https://doi.org/10.1016/j.ygeno.2019.04.016>.
- Layeghifard, M., Hwang, D.M., Guttman, D.S., 2017. Disentangling interactions in the microbiome: a network perspective. *Trends Microbiol.* 25, 217–228. <https://doi.org/10.1016/j.tim.2016.11.008>.
- Liu, C.M., Kachur, S., Dwan, M.G., Abraham, A.G., Aziz, M., Hsueh, P.R., Huang, Y.T., Busch, J.D., Lamit, L.J., Gehring, C.A., Keim, P., Price, L.B., 2012. FungiQuant: a broad-coverage fungal quantitative real-time PCR assay. *BMC Microbiol.* 12 <https://doi.org/10.1186/1471-2180-12-255>.
- Liu, X.M., Chen, K., Meng, C., Zhang, L., Zhu, J.C., Huang, X., Li, S.P., Jiang, J.D., 2014. *Pseudoxanthobacter liyangensis* sp. nov., isolated from dichlorodiphenyltrichloroethane-contaminated soil. *Int. J. Syst. Evol. Microbiol.* 64, 3390–3394. <https://doi.org/10.1099/ij.s.0056507-0>.
- Lopes da Silva, T., Santos, A.R., Gomes, R., Reis, A., 2018. Valorizing fish canning industry by-products to produce ω-3 compounds and biodiesel. *Environ. Technol. Innovat.* 9, 74–81. <https://doi.org/10.1016/j.eti.2017.11.002>.
- Lorini, L., di Re, F., Majone, M., Valentino, F., 2020. High rate selection of PHA accumulating mixed cultures in sequencing batch reactors with uncoupled carbon and nitrogen feeding. *Nat. Biotechnol.* 56, 140–148. <https://doi.org/10.1016/j.nbt.2020.01.006>.
- Marang, L., van Loosdrecht, M.C.M., Kleerebezem, R., 2016. Combining the enrichment and accumulation step in non-axenic PHA production: cultivation of *Plasticumulans acidivorans* at high volume exchange ratios. *J. Biotechnol.* 231, 260–267. <https://doi.org/10.1016/j.jbiotec.2016.06.016>.
- Md Din, M.F., Ujang, Z., van Loosdrecht, M.C.M., Ahmad, A., Sairan, M.F., 2006. Optimization of nitrogen and phosphorus limitation for better biodegradable plastic production and organic removal using single fed-batch mixed cultures and renewable resources. *Water Sci. Technol.* 53, 15–20. <https://doi.org/10.2166/wst.2006.164>.
- Moreira Vieira, N., Zandonade Ventorim, R., de Moura Ferreira, M.A., Barcelos de Souza, G., Menezes de Almeida, E.L., Pereira Vidigal, P.M., Nunes Nesi, A., Gomes Fietto, L., Batista da Silveira, W., 2020. Insights into oleaginous phenotype of the yeast *Papiliotrema laurentii*. *Fungal Genet. Biol.* 144, 103456 <https://doi.org/10.1016/j.fgb.2020.103456>.
- Muzzer, G., De Waal, E.C., Uitterlinden, A.G., 1993. Profiling of complex microbial populations by denaturing gradient gel electrophoresis analysis of polymerase chain reaction-amplified genes coding for 16S rRNA. *Appl. Environ. Microbiol.* 59, 695–700. <https://doi.org/10.1128/aem.59.3.695-700.1993>.
- Oliveira, C.S.S., Silva, C.E., Carvalho, G., Reis, M.A., 2017. Strategies for efficiently selecting PHA producing mixed microbial cultures using complex feedstocks: feast and famine regime and uncoupled carbon and nitrogen availabilities. *Nat. Biotechnol.* 37, 69–79. <https://doi.org/10.1016/j.nbt.2016.10.008>.
- Panagopoulos, A., 2021. Beneficiation of saline effluents from seawater desalination plants: fostering the zero liquid discharge (ZLD) approach - a techno-economic evaluation. *J. Environ. Chem. Eng.* 9, 105338 <https://doi.org/10.1016/j.jece.2021.105338>.
- Panagopoulos, A., Haralambous, K.J., 2020a. Minimal Liquid Discharge (MLD) and Zero Liquid Discharge (ZLD) strategies for wastewater management and resource recovery-Analysis, challenges and prospects. *J. Environ. Chem. Eng.* 8, 104418 <https://doi.org/10.1016/j.jece.2020.104418>.
- Panagopoulos, A., Haralambous, K.J., 2020b. Environmental impacts of desalination and brine treatment - challenges and mitigation measures. *Mar. Pollut. Bull.* 161, 111773 <https://doi.org/10.1016/j.marpolbul.2020.111773>.

- Patel, A., Matsakas, L., 2019. A comparative study on de novo and ex novo lipid fermentation by oleaginous yeast using glucose and sonicated waste cooking oil. *Ultrason. Sonochem.* 52, 364–374. <https://doi.org/10.1016/j.ultsonch.2018.12.010>.
- Patel, A., Pruthi, V., Pruthi, P.A., 2019. Innovative screening approach for the identification of triacylglycerol accumulating oleaginous strains. *Renew. Energy* 135, 936–944. <https://doi.org/10.1016/j.renene.2018.12.078>.
- Pozo, G., Villamar, A.C., Martínez, M., Vidal, G., 2011. Polyhydroxyalkanoates (PHA) biosynthesis from kraft mill wastewaters: biomass origin and C:N relationship influence. *Water Sci. Technol.* 63, 449–455. <https://doi.org/10.2166/wst.2011.242>.
- Qian, X., Li, H., Wang, Y., Wu, B., Wu, M., Chen, L., Li, X., Zhang, Y., Wang, X., Shi, M., Zheng, Y., Guo, L., Zhang, D., 2019. Leaf and root endospheres harbor lower fungal diversity and less complex fungal Co-occurrence patterns than rhizosphere. *Front. Microbiol.* 10, 1–15. <https://doi.org/10.3389/fmicb.2019.01015>.
- Qian, X., Zhou, X., Chen, L., Zhang, X., Xin, F., Dong, W., Zhang, W., Ochsenschreiter, K., Jiang, M., 2021. Bioconversion of volatile fatty acids into lipids by the oleaginous yeast *Apiotrichum porosum* DSM27194. *Fuel* 290, 119811. <https://doi.org/10.1016/j.fuel.2020.119811>.
- Riedel, S.L., Jahns, S., Koenig, S., Bock, M.C.E., Brigham, C.J., Bader, J., Stahl, U., 2015. Polyhydroxyalkanoates production with *Ralstonia eutropha* from low quality waste animal fats. *J. Biotechnol.* 214, 119–127. <https://doi.org/10.1016/j.jbiotec.2015.09.002>.
- Sánchez Valencia, A.I., Rojas Zamora, U., Meraz Rodríguez, M., Álvarez Ramírez, J., Salazar Peláez, M.L., Fajardo Ortiz, C., 2021. Effect of C/N ratio on the PHA accumulation capability of microbial mixed culture fed with leachates from the organic fraction of municipal solid waste (OFMSW). *J. Water Proc. Eng.* 40 <https://doi.org/10.1016/j.jwpe.2021.101975>.
- Sangkharkar, K., Paichid, N., Yunu, T., Klomkiao, S., Prasertsan, P., 2020. Utilisation of tuna condensate waste from the canning industry as a novel substrate for polyhydroxyalkanoate production. *Biomass Conv. Bioref.* <https://doi.org/10.1007/s13399-019-00581-4>.
- Serafim, L.S., Lemos, P.C., Oliveira, R., Reis, M.A.M., 2004. Optimization of polyhydroxybutyrate production by mixed cultures submitted to aerobic dynamic feeding conditions. *Biotechnol. Bioeng.* 87, 145–160. <https://doi.org/10.1002/bit.20085>.
- Silva, F., Campanari, S., Matteo, S., Valentino, F., Majone, M., Villano, M., 2017. Impact of nitrogen feeding regulation on polyhydroxyalkanoates production by mixed microbial cultures. *Nat. Biotechnol.* 37, 90–98. <https://doi.org/10.1016/j.nbt.2016.07.013>.
- Silva, J.B., Pereira, J.R., Marreiros, B.C., Reis, M.A.M., Freitas, F., 2021. Microbial production of medium-chain length polyhydroxyalkanoates. *Process Biochem.* 102, 393–407. <https://doi.org/10.1016/j.procbio.2021.01.020>.
- Smith, D.P., Kock, J.L.F., van Wyk, P.W.J., Pohl, C.H., van Heerden, E., Botes, P.J., Nigam, S., 2003. Oxylipins and ascospore morphology in the ascomycetous yeast genus *Dipodascus*. *Antonie van Leeuwenhoek. Int. J. Gen. Mol. Microbiol.* 83, 317–325. <https://doi.org/10.1023/A:1023340900369>.
- Smolders, G.J.F., van der Meij, J., van Loosdrecht, M.C.M., Heijnen, J.J., 1994. Stoichiometric model of the aerobic metabolism of the biological phosphorus removal process. *Biotechnol. Bioeng.* 44, 837–848. <https://doi.org/10.1002/bit.260440709>.
- Song, J.H., Jeon, C.O., Choi, M.H., Yoon, S.C., Park, W., 2008. Polyhydroxyalkanoate (PHA) production using waste vegetable oil by *Pseudomonas* sp. strain DR2. *J. Microbiol. Biotechnol.* 18, 1408–1415.
- Surendran, A., Lakshmanan, M., Chee, J.Y., Sulaiman, A.M., Thuoc, D. Van, Sudesh, K., 2020. Can polyhydroxyalkanoates Be produced efficiently from waste plant and animal oils? *Front. Bioeng. Biotechnol.* 8 <https://doi.org/10.3389/fbioe.2020.00169>.
- Takahashi, S., Tomita, J., Nishioka, K., Hisada, T., Nishijima, M., 2014. Development of a prokaryotic universal primer for simultaneous analysis of Bacteria and Archaea using next-generation sequencing. *PLoS One* 9. <https://doi.org/10.1371/journal.pone.0105592>.
- Tamis, J., Sorokin, D.Y., Jiang, Y., Van Loosdrecht, M.C.M., Kleerebezem, R., 2015. Lipid recovery from a vegetable oil emulsion using microbial enrichment cultures. *Biotechnol. Biofuels* 8, 1–11. <https://doi.org/10.1186/s13068-015-0228-9>.
- Valentino, F., Beccari, M., Fraraccio, S., Zanolli, G., Majone, M., 2014. Feed frequency in a Sequencing Batch Reactor strongly affects the production of polyhydroxyalkanoates (PHAs) from volatile fatty acids. *Nat. Biotechnol.* 31, 264–275. <https://doi.org/10.1016/j.nbt.2013.10.006>.
- Vastano, M., Corrado, I., Sannia, G., Solaiman, D.K.Y., Pezzella, C., 2019. Conversion of no/low value waste frying oils into biodiesel and polyhydroxyalkanoates. *Sci. Rep.* 9, 1–8. <https://doi.org/10.1038/s41598-019-50278-x>.
- Wallace, T., Gibbons, D., O'Dwyer, M., Curran, T.P., 2017. International evolution of fat, oil and grease (FOG) waste management – a review. *J. Environ. Manag.* 187, 424–435. <https://doi.org/10.1016/j.jenvman.2016.11.003>.
- Waller, J.L., Green, P.G., Loge, F.J., 2012. Mixed-culture polyhydroxyalkanoate production from olive oil mill pomace. *Bioresour. Technol.* 120, 285–289. <https://doi.org/10.1016/j.biortech.2012.06.024>.
- Wang, Y.J., Hua, F.L., Tsang, Y.F., Chan, S.Y., Sin, S.N., Chua, H., Yu, P.H.F., Ren, N.Q., 2007. Synthesis of PHAs from waste under various C:N ratios. *Bioresour. Technol.* 98, 1690–1693. <https://doi.org/10.1016/j.biortech.2006.05.039>.
- Wen, Q., Liu, S., Liu, Y., Chen, Z., 2021. Effect of inoculum and organic loading on mixed culture polyhydroxyalkanoate production using crude glycerol as the substrate. *Int. J. Biol. Macromol.* 182, 1785–1792. <https://doi.org/10.1016/j.ijbiomac.2021.05.184>.
- Yamaguchi, T., Tsuchiya, T., Nakahara, S., Fukui, A., Nagamoto, Y., Murotani, K., Eshima, K., Takahashi, N., 2016. Efficacy of left atrial voltage-based catheter ablation of persistent atrial fibrillation. *J. Cardiovasc. Electrophysiol.* 27, 1055–1063. <https://doi.org/10.1111/jce.13019>.
- Yan, X., Li, D., Ma, X., Li, J., 2021. Bioconversion of renewable lignocellulosic biomass into multicomponent substrate via pressurized hot water pretreatment for bioplastic polyhydroxyalkanoate accumulation. *Bioresour. Technol.* 339, 125667 <https://doi.org/10.1016/j.biortech.2021.125667>.
- Yan, Y., Yang, J., Dou, Y., Chen, M., Ping, S., Peng, J., Lu, W., Zhang, W., Yao, Z., Li, H., Liu, W., He, S., Geng, L., Zhang, X., Yang, F., Yu, H., Zhan, Y., Li, D., Lin, Z., Wang, Y., Elmerich, C., Lin, M., Jin, Q., 2008. Nitrogen fixation island and rhizosphere competence traits in the genome of root-associated *Pseudomonas stutzeri* A1501. *Proc. Natl. Acad. Sci. U. S. A.* 105, 7564–7569. <https://doi.org/10.1073/pnas.0801093105>.
- Yousefi, S.R., Ghanbari, M., Amiri, O., Marzhooseyni, Z., Mehdizadeh, P., Hajizadeh-Oghaz, M., Salavati-Niasari, M., 2021. Dy2BaCuO5/Ba4DyCu3O9.09 S-scheme heterojunction nanocomposite with enhanced photocatalytic and antibacterial activities. *J. Am. Ceram. Soc.* 104, 2952–2965. <https://doi.org/10.1111/jace.17696>.
- Zeng, S., Song, F., Lu, P., He, Q., Zhang, D., 2018. Improving PHA production in a SBR of coupling PHA-storing microorganism enrichment and PHA accumulation by feed-on-demand control. *AMB Express* 8. <https://doi.org/10.1186/s13568-018-0628-x>.